

SCIENTIFIC REPORTS

OPEN

Thermal post-treatment alters nutrient release from a controlled-release fertilizer coated with a waterborne polymer

Received: 28 April 2015
Accepted: 05 August 2015
Published: 08 September 2015

Zijun Zhou^{1,3}, Changwen Du¹, Ting Li^{1,2,3}, Yazhen Shen¹ & Jianmin Zhou¹

Controlled-release fertilizers (CRF) use a controlled-release technology to enhance the nutrient use efficiency of crops. Many factors affect the release of nutrients from the waterborne polymer-coated CRF, but the effects of thermal post-treatments remain unclear. In this study, a waterborne polyacrylate-coated CRF was post-treated at different temperatures (30 °C, 60 °C, and 80 °C) and durations (2, 4, 8, 12, and 24 h) after being developed in the Wurster fluidized bed. To characterize the polyacrylate membrane, and hence to analyze the mechanism of nutrient release, Fourier transform mid-infrared spectroscopy, scanning electron microscopy, and atomic force microscopy were employed. The nutrient-release model of CRF post-treated at 30 °C was the inverse “L” curve, but an increased duration of the post-treatment had no effect. The nutrient-release model was “S” curve and nutrient-release period was enhanced at higher post-treatment temperatures, and increased post-treatment duration lengthened slowed release due to a more compact membrane and a smoother membrane surface as well as a promoted crosslinking action. CRF equipped with specified nutrient-release behaviors can be achieved by optimizing the thermal post-treatment parameters, which can contribute to the development and application of waterborne polymer-coated CRF and controlled-release technologies.

Controlled-release technology has become popular in recent decades, especially in the pharmaceutical industry and agriculture^{1–3}. In agriculture, the technology is mainly used for fertilizers and pesticides⁴. Currently, food security is a worldwide issue as a result of exponential population growth and diminishing areas of arable land^{5,6}. To maintain or enhance crop yields per hectare, excessive fertilizer is often applied, but this has seriously impacted the environment, human health, energy and resource conservation targets, and it constrains sustainable agricultural development^{7,8}.

Controlled-released fertilizers (CRF) enhance nutrient use efficiency, reduce labor costs associated with fertilization, minimize negative toxic effects of excessive fertilization, and aim to supply available nutrients to coincide with plant demand for a long controlled-release period^{9,10}. There are many factors in controlled-release technology that affect the mechanism of nutrient release. The coating materials and the coating process are two key factors that contribute to either a “sudden release” or a “diffusion release” of nutrients from the CRF^{11,12}.

Sulfur and polymer are two kinds of coating materials for CRF on a commercial scale, and they have been used by many organizations, such as Tennessee Valley Authority in USA, Agrium Inc. in Canada, Haifa Chemicals Co. Ltd. in Israel, and Shandong Kingenta Ecological Engineering Co. Ltd. in China^{13–16}. However, compared with sulfur coated CRF, polymer-coated CRF have recently become

¹State Key Laboratory of Soil and Sustainable Agriculture, Institute of Soil Science, Chinese Academy of Sciences, Nanjing 210008, China. ²College of Resources, Sichuan Agricultural University, Chengdu 611130, China. ³University of Chinese Academy of Sciences, Beijing 100049, China. Correspondence and requests for materials should be addressed to C.W.D. (email: chwdu@issas.ac.cn)

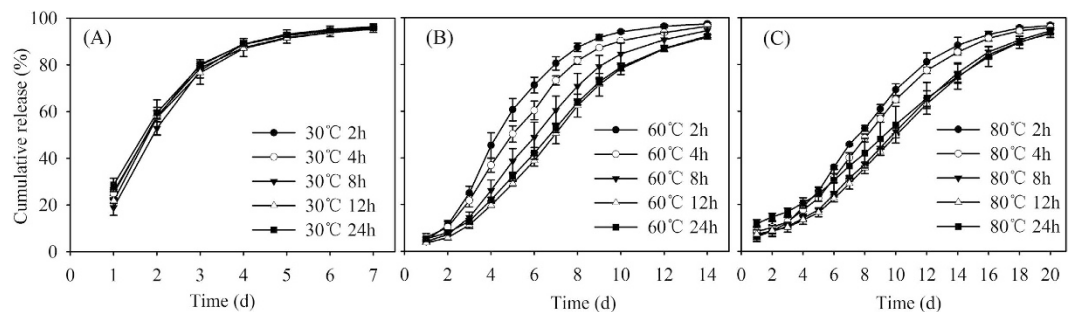


Figure 1. Cumulative nutrient-release profiles from the controlled-release urea post-treated at 30°C (A), 60°C (B), and 80°C (C) for 2, 4, 8, 12, and 24 h, factorially, over the incubation time at 25°C in static distilled water. Bars indicate standard error of the mean ($n = 3$). Treatment details are given in Methods.

more commercially successful due to their improved controlled-release rate, release time, and release pattern^{17,18}. Furthermore, in comparison with the traditional organic coating, waterborne polymer-coated materials are economical, of high quality, safe to use, and environmentally friendly^{2,19,20}.

The Wurster fluidized bed is preferred coating machine over the pan, rotary drum, and conventional fluidized beds because it produces high-quality, rapidly drying CRF of uniform thickness¹². There are more than 20 operational parameters involved in the Wurster fluidized bed coating process²¹, and some of the key parameters in the spray coating process have been analyzed (e.g., spray rate of the polymer latex, fluidization air velocity, atomizing gas flow rate, and gas temperature) and found to significantly affect coating morphology and quality, which in turn affect the behavior of the CRF^{12,22}.

Optimization of the thermal post-treatment parameters after the polymer coating process is still necessary. However, to the best of our knowledge, there is little information on the thermal post-treatment parameters for waterborne polymer-coated CRF, except for Zhao *et al.*¹⁹ who found that higher temperatures strengthened the hydrophobicity of the CRF model membrane which was developed statically in an oven. In our current study, the objective was to examine the effects of thermal post-treated parameters on the nutrient-release behavior of a waterborne polyacrylate-coated CRF. The CRF was produced in a Wurster fluidized bed and then post-treated in a convection oven. Nutrient release from the CRF was detected in distilled water, and the membrane changes were observed using Fourier transform mid-infrared spectroscopy (FT-IR), scanning electron microscopy (SEM), and electron digital caliper and atomic force microscopy (AFM).

Results

Nutrient release from the polymer-coated CRF. The profiles of nutrient release into distilled water from the post-treated CRF at 30°C, 60°C, and 80°C for 2, 4, 8, 12, and 24 h, factorially, are shown in Fig. 1. The fastest nutrient release occurred for the 30°C post-treatment with an 80% cumulative release at 3 d, and increased post-treatment time did not significantly change the nutrient release. Higher post-treatment temperatures (60°C and 80°C) slowed the controlled release, and changed the release model from the inverse “L” curve at 30°C to the “S” curve at both 60°C and 80°C. The cumulative release reached 80% at about 7, 8, 9, and 10 d for the 60°C post-treatment applied for 2, 4, 8, and 12 h, respectively; the 24 h post-treatment did not extend the duration of release. The cumulative release reached 80% at 12 d for the 80°C post-treatments applied for 2 and 4 h, and at about 15 d for post-treatments applied for 8, 12, and 24 h.

Membrane characteristics of the polymer-coated CRF. During the Wurster fluidized bed procedure, waterborne polymer emulsion was sprayed onto the surface of the round urea granules to form a coating that was immediately dried. Repeated spraying of the emulsion and then drying built a membrane coating around the granules^{12,22} (Fig. 2).

The FT-IR was used to detect the composition of the coating membrane. The FT-IR spectra of the coating membranes had several similar functional groups: O–H and N–H stretching vibration (3250–3550 cm^{-1}), C–H stretching vibration ($\sim 2850 \text{ cm}^{-1}$), C=O stretching vibration ($\sim 1730 \text{ cm}^{-1}$), C–H bend vibration ($\sim 1450 \text{ cm}^{-1}$), and C–O stretching vibration ($\sim 1160 \text{ cm}^{-1}$) (Fig. 3). However, there were some differences among the spectra. Calculations were made for the profiling depth of the membranes:

$$\mu = \sqrt{\frac{D}{\pi v \gamma}} \quad (1)$$

where μ is the profiling depth (μm), D is the thermal diffusivity of sample ($\text{m}^2 \text{ s}^{-1}$), v is the moving mirror velocity (cm s^{-1}), and γ is the wavenumber (cm^{-1})²³. The profiling depths (μm) were calculated

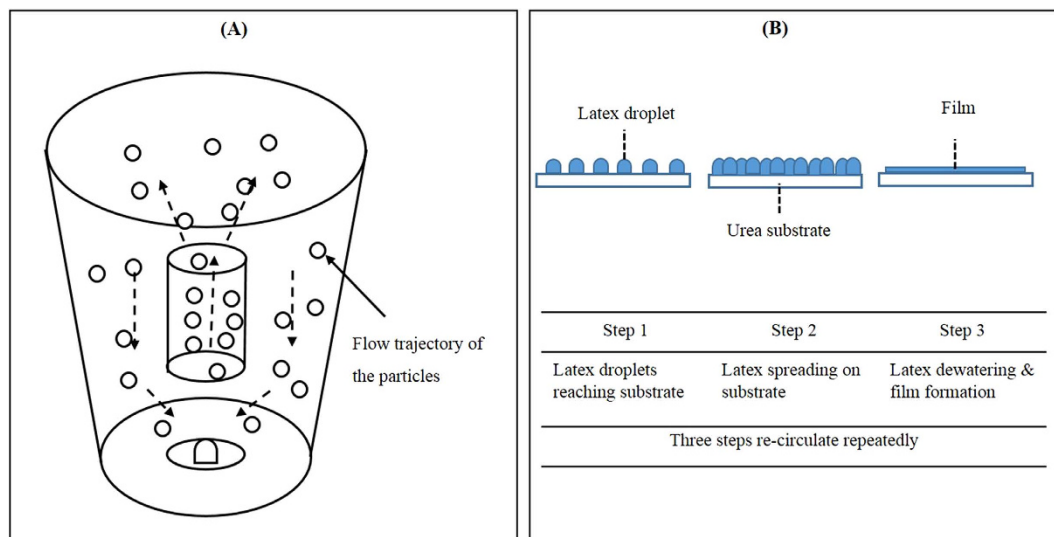


Figure 2. Schematic of the spray coating process in a Wurster fluidized bed¹² (A) and film formation in the spray coating process²² (B).

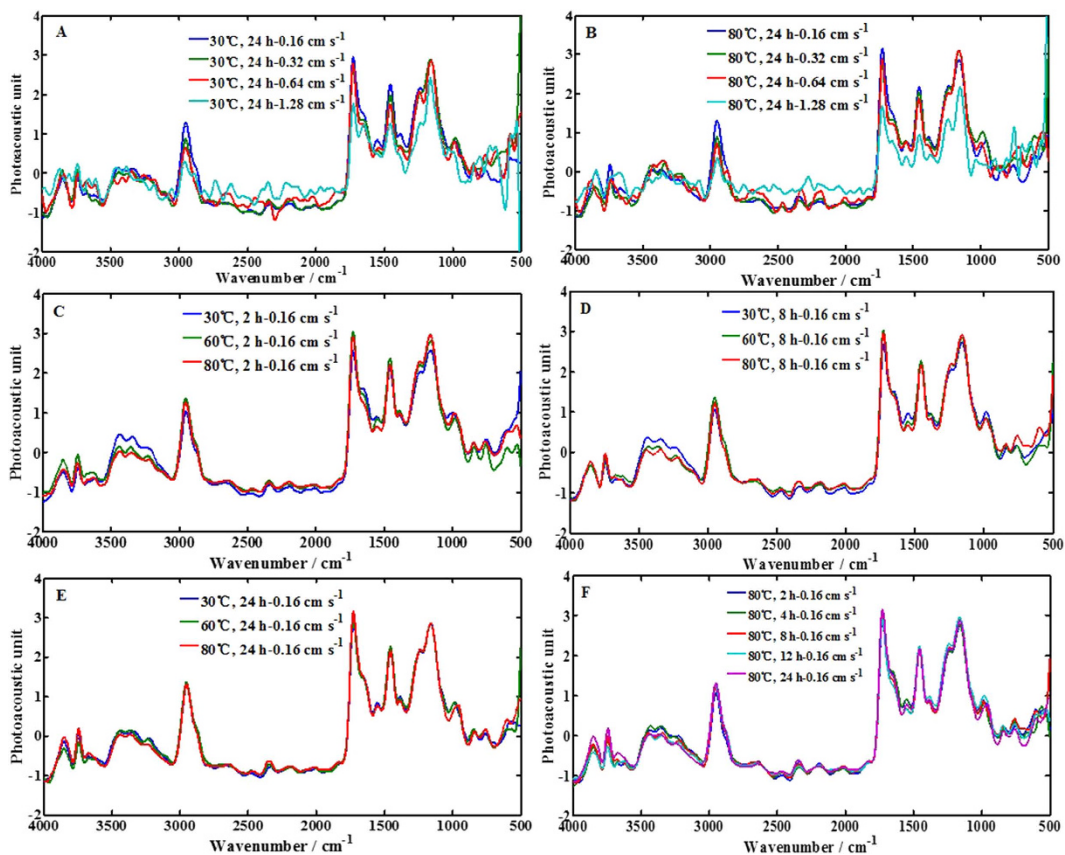


Figure 3. FT-IR spectra of the coating membranes from the waterborne polyacrylate-coated CRF under different post-treated temperatures and times. (A,B), spectra of membranes at four mirror velocities post-treated under 30°C (A) and 80°C (B) for 24 h each; (C–F), spectra of CRF membranes at 0.16 cm s^{-1} moving mirror velocity that were post-treated at three temperatures (30°C, 60°C, and 80°C) for 2 h (C), 8 h (D), and 24 h (E), and at 80°C for five durations (2, 4, 8, 12, and 24 h) (F).

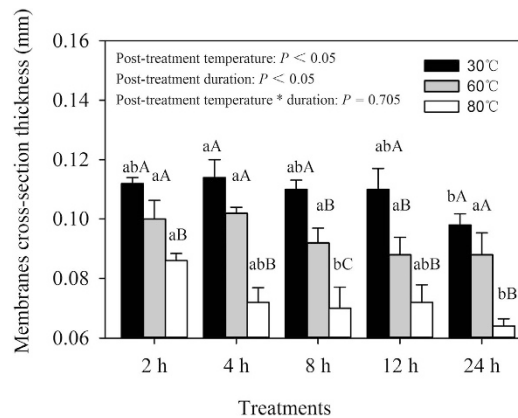


Figure 4. Cross-section thickness of the polymer membrane on the CRF post-treated at 30 °C, 60 °C, and 80 °C for 2, 4, 8, 12, and 24 h, factorially. Bars indicate standard error of the mean ($n = 5$). Treatment details are given in Methods. Values with different lowercase letters are different at a significance level of $P < 0.05$ for each post-treatment temperature. Values with different uppercase letters are different at a significance level of $P < 0.05$ for each post-treatment duration. The interaction between post-treatment temperature and duration had no significant effect on membrane cross-section thickness ($P = 0.705$).

at four different moving-mirror velocities (0.16, 0.32, 0.64, and 1.28 cm s^{-1}), whereby 0.16 cm s^{-1} was the deepest layer, and 1.28 cm s^{-1} was the outermost layer. The coating membrane was heterogeneous (Fig. 3A,B). Membrane hydrophobicity was a key factor affecting the nutrient-release pattern from the CRF, and it was generally acknowledged that waterborne polymer coated CRF with higher membrane hydrophobicity had a longer controlled period of nutrient-release^{19,24}. The hydrophilic groups, such as the $-\text{OH}$ and $-\text{NH}$, and the hydrogen bond acceptors, such as the carbonyl of ester, facilitated moisture uptake. The ratio of intensity of hydrophobic group ($-\text{CH}$) to the intensity of hydrophilic group (e.g., $-\text{NH}$, $-\text{OH}$, and $-\text{C}=\text{O}$) could be used to reveal the hydrophobicity of the membrane¹⁹. Therefore, spectra at 0.16 cm s^{-1} were further used for their high signal-to-noise ratio and high hydrophobicity. Figure 3C–E show the changes in the membrane spectra during the post-treatments at 30 °C, 60 °C, and 80 °C, respectively. From the spectra, the membranes post-treated at 30 °C showed the largest intensity of hydrophilic group (e.g., $-\text{NH}$, $-\text{OH}$, and $-\text{C}=\text{O}$) with the least intensity of hydrophobic group ($-\text{CH}$) in three post-treated temperatures, which meant membranes post-treated at 30 °C was the least hydrophobic in three temperatures for the 2 h and 8 h of post-treatment duration; and hydrophobicity of membranes post-treated at 80 °C was slightly higher than that at 60 °C. The hydrophobicity of the membranes exposed to different post-treatment temperatures became more similar as the post-treatment duration increased, which was attributed to the both the time necessary to complete the crosslinking action (about 1 d at room temperature)²⁵, and the high temperature to accelerate the action. Figure 3F shows that lower intensity of hydrophilic group (e.g., $-\text{NH}$, $-\text{OH}$, and $-\text{C}=\text{O}$) and higher intensity of hydrophobic group ($-\text{CH}$) resulted from increased thermal post-treated duration at post-treated temperature of 80 °C, which means the crosslinking action needed time for completion.

An electron digital caliper and SEM were employed to reveal the cross-section structure of the coating membrane. Figure 4 shows that using an electron digital caliper, the cross-section thickness of the coating membrane decreased as the post-treatment temperature and duration increased. The CRF post-treatment at 30 °C for 2 h was the thickest (~ 0.11 mm), whereas that treated at 80 °C for 24 h was the thinnest (~ 0.07 mm). Using SEM, we examined coating membranes post-treated at 30 °C, 60 °C, and 80 °C for 2 h and 8 h each, to demonstrate cross-section morphological structures (Fig. 5). The membrane cross-section thickness of CRF post-treated at 30 °C was the thickest (~ 0.085 mm), whereas that at 80 °C for 8 h was the thinnest (~ 0.055 mm). The trends for the cross-section thicknesses in response to increased post-treatment temperature and duration were similar between the two measurement methods, although the electron digital caliper indicated thicker membranes than those measured using SEM. This might be attributed to inconsistent whole membrane thickness, or fertilizer dust adhering to the membrane. Furthermore, cross-sections of membranes post-treated at 30 °C for 2 h showed the largest number of pores, whereas no observable pores were observed in cross-sections of membranes post-treated at 80 °C. Therefore, the pore size and pore density of the post-treated membranes significantly decreased with an increase in post-treatment temperature and duration, and increased temperature significantly compacted the coating membrane.

AFM measurements were used to study the surface morphology of membranes from a CRF post-treated at 30 °C, 60 °C, and 80 °C for 2 h and 8 h, respectively. Figure 6 shows the three dimensional height images (A–F) and phase images (a–f) from AFM. It can be clearly observed from the three dimensional height images as well as the phase images that the membranes post-treated at 60 °C and 80 °C were smoother than those at 30 °C. Table 1 represents the average roughness (R_a), root mean square roughness (R_q),

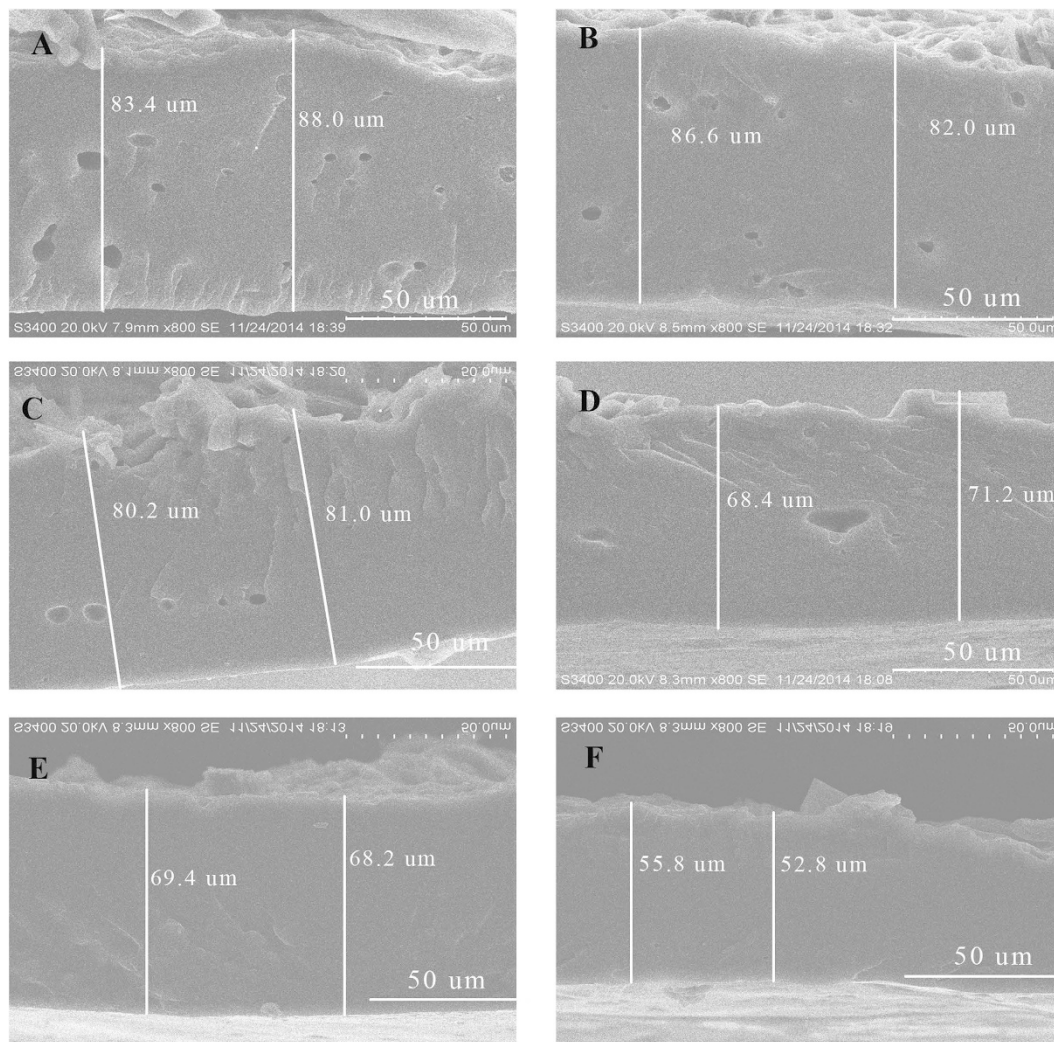


Figure 5. Cross-section images of coating membranes from waterborne polyacrylate-coated CRF under different post-treatment temperatures and durations using a scanning electron microscopy (SEM). (A–F), membranes of post-treatments at 30°C 2 h (A), 30°C 8 h (B), 60°C 2 h (C), 60°C 8 h (D), 80°C 2 h (E), and 80°C 8 h (F), respectively.

and maximum roughness (R_{max}), which were calculated using AFM software (NanoScope Analysis). There was a similar decreasing trend in membrane R_a , R_q , and R_{max} from a CRF post-treated at 30°C for 2 h and 8 h, 60°C for 2 h and 8 h, and 80°C for 2 h and 8 h. Membranes post-treated at 30°C were the roughest, whereas membrane roughness was no different between 60°C and 80°C. Higher temperatures may contribute to polymer remodeling, and lead to more compact membranes with smoother surfaces.

Discussion

The type of coating material and the coating technology are both responsible for the mechanism of nutrient release from controlled-release fertilizers^{11,12}. In this study, we concluded that thermal post-treatment parameters were closely related to the nutrient-release behavior of the waterborne polymer-coated CRF. The temperature of the fluidizing gas must be high enough to evaporate the solvent, and to prevent aggregation of the coated particles, and it also should be below an upper-temperature (e.g., polymer-softening temperature) to avoid massive aggregation¹³. Lan *et al.*²² found that the gas temperature significantly affected the film surface morphology and that sprayed films prepared at 35°C were smooth, and enhanced gas permeability led to more porous structures in the films, which resulted in increased film permeability coefficients when the gas temperature was higher than 40°C. Thompson and Kelch²⁶ reported that process temperatures that were 20°C–30°C higher than the latex glass temperature was suitable for the formation of a dense and uniform film. Therefore, in our study, a gas temperature of about 35°C was adopted to develop the CRF in the Wurster fluidized bed.

Kong *et al.*²⁷ and Pacheco *et al.*²⁸ found that membrane structural factors (thickness, pore size, surface area, and roughness) and chemical properties (hydrophilicity or hydrophobicity) affected the water

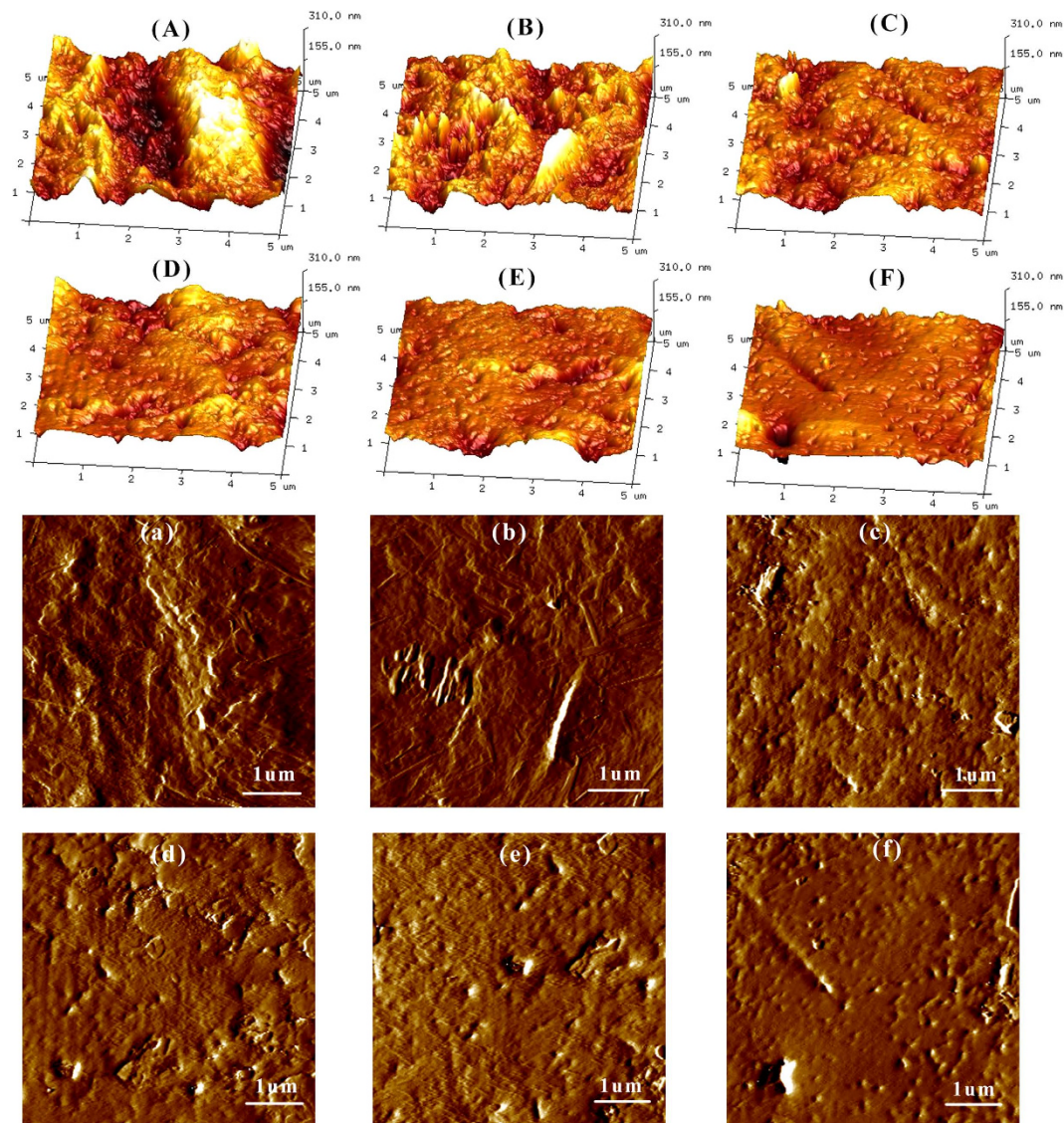


Figure 6. Surface morphological structures of membranes from CRF post-treated at 30°C, 60°C, and 80°C for 2 h and 8 h, factorially. (A–F): height images of membranes post-treated at 30°C for 2 h (A), 30°C for 8 h (B), 60°C for 2 h (C), 60°C for 8 h (D), 80°C for 2 h (E), and 80°C for 8 h (F); a–f: phase images of membranes post-treated at 30°C for 2 h (a), 30°C for 8 h (b), 60°C for 2 h (c), 60°C for 8 h (d), 80°C for 2 h (e), and 80°C for 8 h (f).

Post-treatment temperatures	Ra (nm)		Rq (nm)		Rmax (nm)	
	2 h	8 h	2 h	8 h	2 h	8 h
30°C	30.1 ± 3.7A	25.8 ± 3.7A	39.6 ± 3.5A	33.5 ± 4.9A	281.3 ± 10.7A	284.0 ± 44.0A
60°C	12.9 ± 1.4B	12.5 ± 1.5B	17.2 ± 1.5B	16.9 ± 1.7B	152.7 ± 13.3B	159.7 ± 7.1B
80°C	14.0 ± 1.4B	12.1 ± 2.3B	16.9 ± 2.7B	16.0 ± 3.2B	161.2 ± 44.3B	160.6 ± 35.6B

Table 1. Surface roughness (Mean ± Standard Error of Mean, n = 3) of the membranes from the CRF post-treated at 30°C, 60°C, and 80°C for 2 and 8 h, factorially, by atomic force microscopy (AFM). Ra: average roughness; Rq: root mean square roughness; Rmax: maximum roughness. Values with different letters are different at a significance level of $P < 0.05$ for each post-treatment duration. The different post-treatment durations had no significant effect on membrane Ra ($P = 0.219$), Rq ($P = 0.270$) and Rmax ($P = 0.883$), respectively. The interaction between post-treatment temperature and duration had no significant effect on membrane Ra ($P = 0.649$), Rq ($P = 0.489$) and Rmax ($P = 0.988$), respectively.

flux. The hydrophobicity mainly depended on the following factors: hydrophilic groups present in the polymer, Vander Waals' interaction in terms of hydrogen bonding, average molecular interchain structure, and hydrophobicity of the alkyl chain length²⁹. These are possible reasons for the different release behaviors from the CRF exposed to various post-treatments.

For the CRF post-treatment at 30 °C, abundant pores in the membrane cross-section contributed to the water molecules quickly moving into the CRF coating and to the easy release of small urea molecules from the pores, which resulted in a high rate of nutrient release. High surface roughness of the membrane also led to low hydrophobicity³⁰ and increased water contact with the higher surface area of the membrane³¹, which also accelerated nutrient release. Post-treatment duration did not affect the controlled-release behavior, mainly because pore size and membrane cross-section thickness did not change significantly at the relative low temperature; although aziridine ring groups of the cross-linker can react with –COOH in waterborne polyacrylate emulsion at room temperature (e.g., 30 °C).

For CRF post-treatment at 60 °C and 80 °C, the pore density in the membrane cross-section, the surface roughness of the membrane were all reduced significantly compared with CRF post-treated at 30 °C. This contributed to changing the nutrient controlled-release model from inverse “L” curve to “S” curve and prolonging the nutrient-release period. With an increase in post-treatment duration (from 2 h to 8 h) at 60 °C, pore density and the cross-section thickness of the membrane reduced significantly, which led to a compact membrane, which slowed the nutrient release.

Nutrient-release from the CRF post-treated at both 60 °C and 80 °C slowed with an increase in the post-treatment duration, but there was no additional slowing of nutrient release at 60 °C after 12 h or at 80 °C after 8 h of the post-treatment, which may be attributed to the completion of crosslinking action and polymer remodeling. Compared with CRF post-treated at 30 °C and 60 °C, there were several reasons for the slower nutrient release for the CRF post-treated at 80 °C. Firstly, no pores occurred in the membrane cross-section and the membrane cross-section was the thinnest for this treatment, which meant that the membrane from the CRF post-treated at 80 °C was the most compact. Secondly, the higher temperature promoted crosslinking action and consequently strengthened the membrane hydrophobicity¹⁹, which decreased the ability of water molecules to be absorbed. In addition, high temperature could enhance the mechanical strength of the membrane³², which may reduce the nutrient-release surface area of the swollen CRF.

The different nutrient-release models for CRF under varied post-treated parameters indicated that a higher temperature led to a more compact membrane with less pores in the cross-section and smoother membrane surface, and then might reduce the film diffusivity. CRF equipped with specified nutrient-release behaviors could be achieved by specified adjustments of post-treatment parameters, which could contribute to the development and application of waterborne polymer-coated CRFs and controlled-release technologies.

Methods

Materials. To prepare the CRF, commercial grade urea granules (46.4% nitrogen) were purchased from Luxi Chemical Co. Ltd. (Liaocheng, China), and waterborne polyacrylate emulsion (50% dry matter content), provided by Doctor Hydrophilic Chemicals Co. Ltd. (Yizheng, China), was used as a coating material. The emulsion was polymerized from butyl acrylate, methyl methacrylate, and methyl acrylic acid. The glass transition temperature of the polymer is around 8 °C¹⁹.

Preparation of the polymer-coated CRF. Urea granules (36 kg) were loaded into a pilot scale Wurster fluidized bed (LDP-5, Jiafa Mechanic Co. Ltd., Changzhou, China). The bed temperature was set at 35 ± 5 °C and preheated for 10 min. Waterborne polyacrylate emulsion (8 kg) was diluted with 8 kg water and then mixed with 80 g of the cross-linker aziridine, which was sprayed through a nozzle using a peristaltic pump at the speed of 0.20 L min⁻¹ at an atomizing pressure of 0.4 MPa. A 2 kg batch of coated CRF was stored at 4 °C in a desiccator containing allochroic silica gel^{19,22}.

Characterization of nutrient release from the CRF. The CRF was subdivided into 15 samples, which were post-treated at three temperatures (30 °C, 60 °C, and 80 °C) for five durations (2, 4, 8, 12, and 24 h), factorially. A 10 g sample of CRF granules was placed in a sealed glass bottle with 200 mL of distilled water and then incubated at 25 °C. The nutrient release was measured using the paradimethyl-aminobenzaldehyde colorimetric method every 24 h for the first 10 days and then every 48 h until the end of the experiment. The distilled water in the glass bottle was refreshed after measuring the released nutrients. On the last day of nutrient release, the coated fertilizers were ground to determine the residual nutrients. The nutrient-release profile was estimated as the cumulative release percentage versus the incubation time.

Characterization of the CRF membrane. The post-treated CRF granules were cut into two pieces with a sharp blade, and the coating membranes were removed slightly from the CRF granules with tweezers.

To determine the composition of the coating membranes we used an FT-IR spectrometer (Nicolet 6700, MA, USA) with a photoacoustic accessory (MTEC model 300, IA, USA). The scans were conducted in the mid-IR region (500–4000 cm⁻¹) with a resolution of 4 cm⁻¹ and four mirror velocities of 0.16, 0.32,

0.64, and 1.28 cm s⁻¹, and 32 successive scans were recorded. A glassy carbon reference material was used as the surface absorber to calibrate the system³³.

An AFM (Dimension Edge, Bruker, Germany) was used to study the surface topography of the membranes. The membranes were fixed onto the mica plate and then positioned on top of the scanner tube. The AFM laser beam was focused onto the preselected spot of the surface prior to engaging the cantilever. AFM images were collected in tapping mode with silicone tip cantilevers³⁴.

The cross-section thickness of the coating membranes were measured using an electron digital caliper (Chengliang Tools Group Co. Ltd, Chengdu, China). The cross-section morphology of the coating membranes were examined by SEM (S-3400, Hitachi, Japan) with an accelerating voltage of 20 kV and 95 μA. The coating membranes were fractured in liquid nitrogen and cross-sections of the samples were gold sputtered for 2 min before observation.

Data analyses. All spectral data were processed using Matlab 2009b. The AFM images were analyzed using the NanoScope software (Version 5.12b48). A two-way analysis of variance (ANOVA) was performed to test the primary and interactive effects of the post-treatment temperature and duration on both membrane cross-section thickness (Fig. 4) and membrane roughness (Table 1) using SPSS 16.0. The assumption of homogeneity of variance was tested with Levene's test at $\alpha = 0.05$. When statistically significant differences existed according to ANOVA ($P < 0.05$), treatment means were compared using Duncan test at $\alpha = 0.05$.

References

- Balmayor, E. R., Azevedo, H. S. & Reis, R. L. Controlled delivery systems: from pharmaceuticals to cells and genes. *Pharm. Res.* **28**, 1241–1258 (2011).
- Du, C. W., Shen, Y. Z. & Zhou, J. M. Application of aqueous silicone-acrylate emulsions in coated controlled release fertilizer. *J. Control. Release* **172**, 18–19 (2013).
- Fredenberg, S., Wahlgren, M., Reslow, M. & Axelsson, A. The mechanisms of drug release in poly (lactic-co-glycolic acid)-based drug delivery systems-A review. *Int. J. Pharm.* **415**, 34–52 (2011).
- Watanabe, A., Takebayashi, Y., Ohtsubo, T. & Furukawa, M. Permeation of urea through various polyurethane membranes. *Pest Manag. Sci.* **65**, 1233–1240 (2009).
- Brown, M. E., Hintermann, B. & Higgins, N. Markets, climate change, and food security in West Africa. *Environ. Sci. Technol.* **43**, 8016–8020 (2009).
- Chen, J., Chen, J. Z., Tan, M. Z. & Gong, Z. T. Soil degradation: a global problem endangering sustainable development. *J. Geogr. Sci.* **12**, 243–252 (2002).
- Choudhury, A. T. M. A. & Kennedy, I. R. Nitrogen fertilizer losses from rice soils and control of environmental pollution problems. *Commun. Soil Sci. Plant Anal.* **36**, 1625–1639 (2005).
- Han, X. Z., Chen, S. S. & Hu, X. G. Controlled-release fertilizer encapsulated by starch/polyvinyl alcohol coating. *Desalination* **240**, 21–26 (2009).
- Shaviv, A. Advances in controlled-release fertilizers. *Adv. Agron.* **71**, 1–49 (2001).
- Yang, Y. C., Zhang, M., Li, Y. C., Fan, X. H. & Geng, Y. Q. Controlled release urea improved nitrogen use efficiency, activities of leaf enzymes, and rice yield. *Soil Sci. Soc. Am. J.* **76**, 2307–2317 (2012).
- Tomaszewska, M., Jarosiewicz, A. & Karakulski, K. Physical and chemical characteristics of polymer coatings in CRF formulation. *Desalination* **146**, 319–323 (2002).
- Tzika, M., Alexandridou, S. & Kiparissides, C. Evaluation of the morphological and release characteristics of coated fertilizer granules produced in a Wurster fluidized bed. *Powder Technol.* **132**, 16–24 (2003).
- Du, C., Tang, D., Zhou, J., Wang, H. & Shaviv, A. Prediction of nitrate release from polymer-coated fertilizers using an artificial neural network model. *Biosyst. Eng.* **99**, 478–486 (2008).
- Kiran, J. K., Khanif, Y. M., Amminuddin, H. & Anuar, A. R. Effects of controlled release urea on the yield and nitrogen nutrition of flooded rice. *Commun. Soil Sci. Plant Anal.* **41**, 811–819 (2010).
- McKenzie, R. H., Bremer, E., Middleton, A. B., Pffiffer, P. G. & Dowbenko, R. E. Controlled-release urea for winter wheat in southern Alberta. *Can. J. Soil Sci.* **87**, 85–91 (2007).
- Wilson, M. L., Rosen, C. J. & Monerief, J. F. A comparison of techniques for determining nitrogen release from polymer-coated urea in the field. *Hortscience* **44**, 492–494 (2009).
- Azeem, B., KuShaari, K., Man, Z. B., Basit, A. & Thanh, T. H. Review on materials & methods to produce controlled release coated urea fertilizer. *J. Control. Release* **181**, 11–21 (2014).
- Shaviv, A., Raban, S. & Zaidel, E. Modeling controlled nutrient release from a population of polymer coated fertilizers: statistically based model for diffusion release. *Environ. Sci. Technol.* **37**, 2251–2261 (2003).
- Zhao, C. *et al.* Evaluation of waterborne coating for controlled-release fertilizer using Wurster fluidized bed. *Ind. Eng. Chem. Res.* **49**, 9644–9647 (2010).
- Zhou, Z. J. *et al.* Biodegradation of a biochar-modified waterborne polyacrylate membrane coating for controlled-release fertilizer and its effects on soil bacterial community profiles. *Environ. Sci. Pollut. Res.* **22**, 8672–8682 (2015).
- Mehta, A. M. [Processing and equipment considerations for aqueous coatings]. *Aqueous Polymeric Coatings for Pharmaceutical Dosage Forms*, Third Edition. [McGinity, J. W. & Felton, L. A. (eds.)] [67–103] (CRC Press, Florida, USA, 2008).
- Lan, R. *et al.* Experimental modeling of polymer latex spray coating for producing controlled-release urea. *Particuology* **9**, 510–516 (2011).
- Zhang, W. R., Zhu, T. T., Smith, R. & Lowe, C. Non-destructive study on the degradation of polymer coating I: Step-scan photoacoustic FTIR and confocal Raman microscopy depth profiling. *Polym. Test* **31**, 855–863 (2012).
- Shen, Y. Z., Du, C. W. & Zhou, J. M. Aqueous polyacrylate/poly(silicone-co-acrylate) emulsion coated fertilizers for slow nutrient-release application. *J. Appl. Polym. Sci.* doi: 10.1002/app.40369 (2015).
- Tillet, G., Boutevin, B. & Ameduri, B. Chemical reactions of polymer crosslinking and post-crosslinking at room and medium temperature. *Prog. Polym. Sci.* **36**, 192–217 (2011).
- Thompson H. E. & Kelch R. A. inventors; The O. M. Scott & Sons Company, assignee. Encapsulated slow release fertilizers. United States patent US 5,186, 732. 1993 Feb 16.
- Kong, C. L., Shintani, T., Kamada, T., Freger, V. & Tsuru, T. Co-solvent-mediated synthesis of thin polyamide membranes. *J. Membr. Sci.* **384**, 10–16 (2011).

28. Pacheco, F. A., Pinnau, I., Reinhard, M. & Leckie, J. O. Characterization of isolated polyamide thin films of RO and NF membranes using novel TEM techniques. *J. Membr. Sci.* **358**, 51–59 (2010).
29. Purushothaman, M., Krishnan, P. S. G. & Nayak, S. K. Poly(alkyl lactate acrylate)s having tunable hydrophilicity. *J. Appl. Polym. Sci.* doi: 10.1002/app.40962 (2014).
30. Huang, S. H. *et al.* Study on characterization and pervaporation performance of interfacially polymerized polyamide thin-film composite membranes for dehydrating tetrahydrofuran. *J. Membr. Sci.* **470**, 411–420 (2014).
31. Singh, S., Khulbe, K. C., Matsuura, T. & Ramamurthy, P. Membrane characterization by solute transport and atomic force microscopy. *J. Membr. Sci.* **142**, 111–127 (1998).
32. Yoo, Y. *et al.* Preparation of acrylic copolymers and crosslinking agents and properties as a film. *J. Appl. Polym. Sci.* **112**, 1587–1594 (2009).
33. Du, C. W., Zhou, G. Q., Wang, H. Y., Chen, X. Q. & Zhou, J. M. Depth profiling of clay-xanthan complexes using step-scan mid-infrared photoacoustic spectroscopy. *J. Soils Sediments* **10**, 855–862 (2010).
34. Xiang, Y. H., Xue, L. X., Shen, J. H., Lin, H. B. & Liu, F. Effect of solvents on morphology and polymorphism of polyvinylidene fluoride membrane via supercritical CO₂ induced phase separation. *J. Appl. Polym. Sci.* doi: 10.1002/app.41065 (2014).

Acknowledgements

This study was financially supported by National 12th Five-Year Science and Technology Supporting Program (grant No. 2011BAD11B01-02) and the cooperation project between Chinese Academy of Sciences and local industry (grant No. YDJDBNJ-2012-023).

Author Contributions

C.W.D. and Z.J.Z. initiated and designed the research. Z.J.Z. and T.L. performed the experiments. Z.J.Z. and C.W.D. analysed the data and wrote the paper. T.L., Y.Z.S. and J.M.Z. also revised and edited the manuscript.

Additional Information

Competing financial interests: The authors declare no competing financial interests.

How to cite this article: Zhou, Z. *et al.* Thermal post-treatment alters nutrient release from a controlled-release fertilizer coated with a waterborne polymer. *Sci. Rep.* **5**, 13820; doi: 10.1038/srep13820 (2015).



This work is licensed under a Creative Commons Attribution 4.0 International License. The images or other third party material in this article are included in the article's Creative Commons license, unless indicated otherwise in the credit line; if the material is not included under the Creative Commons license, users will need to obtain permission from the license holder to reproduce the material. To view a copy of this license, visit <http://creativecommons.org/licenses/by/4.0/>